

# Localization of Ceramide and Glucosylceramide in Human Epidermis by Immunogold Electron Microscopy

Gabriele Vielhaber,\*† Stephan Pfeiffer,\*¶ Lore Brade,† Buko Lindner,§ Torsten Goldmann,‡ Ekkehard Vollmer,‡ Ulrich Hintze,\* Klaus-Peter Wittern,\* and Roger Wepf\*

\*Analytical Research Department, Beiersdorf AG, Hamburg, Germany; †Divisions of Medical and Biochemical Microbiology, ‡Clinical and Experimental Pathology, and §Biophysics, Center for Medicine and Biosciences, Research Center Borstel, Borstel, Germany

Ceramides and glucosylceramides are pivotal molecules in multiple biologic processes such as apoptosis, signal transduction, and mitogenesis. In addition, ceramides are major structural components of the epidermal permeability barrier. The barrier ceramides derive mainly from the enzymatic hydrolysis of glucosylceramides. Recently, anti-ceramide and anti-glucosylceramide anti-sera have become available that react specifically with several epidermal ceramides and glucosylceramides, respectively. Here we demonstrate the detection of two epidermal covalently bound  $\omega$ -hydroxy ceramides and one covalently bound  $\omega$ -hydroxy glucosylceramide species by thin-layer chromatography immunostaining. Moreover, we show the ultrastructural distribution of ceramides and glucosylceramides in human epidermis by immunoelectron microscopy on cryoprocessed skin samples. In basal epidermal cells and dermal fibroblasts ceramide was found: (i) at the nuclear envelope; (ii) at the inner and outer mito-

chondrial membrane; (iii) at the Golgi apparatus and the endoplasmic reticulum; and (iv) at the plasma membrane. The labeling density was highest in mitochondria and at the inner nuclear membrane, suggesting an important role for ceramides at these sites. In the upper epidermis, ceramides were localized: (i) in lamellar bodies; (ii) in *trans*-Golgi network-like structures; (iii) at the cornified envelope; and (viii) within the intercellular space of the stratum corneum, which is in line with the known analytical data. Glucosylceramides were detected within lamellar bodies and in *trans*-Golgi network-like structures of the stratum granulosum. The localization of glucosylceramides at the cornified envelope of the first corneocyte layer provides further proof for the existence of covalently bound glucosylceramides in normal human epidermis. **Key words:** cornified envelope/glycosphingolipids/immunostaining/skin barrier. *J Invest Dermatol* 117:1126–1136, 2001

**A**mong sphingolipids, outstanding interest has been dedicated to the biologic functions of ceramides (Cer) and in the recent past also to those of glucosylceramides (GlcCer). Cer are involved in numerous cellular signaling processes in response to extracellular stress, such as apoptosis, terminal differentiation, or cell cycle arrest and growth suppression (reviewed in Geilen *et al*, 1997; Perry and

Hannun, 1998). Cer analogs with natural fatty acid chain lengths (C16–C24) activate several protein kinases (Müller *et al*, 1995; Huwiler *et al*, 1996; Zhang *et al*, 1997), protein phosphatases (Chalfant *et al*, 1999), and the protease cathepsin D (Heinrich *et al*, 1999).

The fate of intracellular Cer has been followed using synthetic Cer short-chain analogs (C2–C6) (Rosenwald and Pagano, 1993) or radiolabeled biosynthetic precursors (Van Echten-Deckert *et al*, 1997), but the sites of Cer compartmentalization are still obscure. Cer *de novo* synthesis takes place at the cytoplasmic leaflet of the endoplasmic reticulum (ER). The lipid can be further metabolized to GlcCer at the cytosolic surface of the *cis*-Golgi cisternae or converted into sphingomyelin, most probably in the Golgi lumen (Jeckel *et al*, 1992). Another source of Cer generation is the hydrolysis of sphingomyelin at the plasma membrane in response to extracellular stimuli, such as tumor necrosis factor- $\alpha$ , interleukin-1, and endotoxin (reviewed in Levade and Jaffrézou, 1999). Cell permeable short chain analogs of Cer accumulate in the Golgi apparatus (Lipsky and Pagano, 1983, 1985), but the various sites of Cer action also suggest a localization near the plasma membrane and the mitochondria (Perry and Hannun, 1998).

GlcCer are important intermediates in glycosphingolipid biosynthesis and markers for multidrug resistant tumors that express enhanced GlcCer levels (Lavie *et al*, 1996; Lucci *et al*, 1998). Moreover, they play an essential part in mitogenesis, epidermal

Manuscript received January 17, 2001; revised May 7, 2001; accepted for publication June 16, 2001.

Reprint requests to: Dr. Gabriele Vielhaber, Haanman & Reimer GmbH, Mühlenfeldstrasse 1, D-37603, Holzminden, Germany. Email: gvvielhaber@telda.net

Abbreviations: Cer, ceramide; GlcCer, glucosylceramide; Cer-1, O-acyl-N-( $\omega$ -hydroxyacyl)-sphingosine; Cer-2, N-acyl-sphingosine; Cer-3, N-acyl-4-hydroxysphinganine; Cer-4, O-acyl-N-( $\omega$ -hydroxyacyl)-6-hydroxysphingosine; Cer-5, N-(2-hydroxyacyl)-sphingosine; Cer-6, N-(2-hydroxyacyl)-4-hydroxysphinganine; Cer-7, N-(2-hydroxyacyl)-6-hydroxysphingosine; Cer A, N-( $\omega$ -hydroxyacyl)-sphingosine; Cer B, N-( $\omega$ -hydroxyacyl)-6-hydroxysphingosine; ER, endoplasmic reticulum; GlcCer-2, 1-O-( $\beta$ -D-glucopyranosyl)-N-acyl-sphingosine; GlcCer-sb, N-(2-hydroxypalmitoyl)-4,8-sphingadienine; LB, lamellar body; MALDI-TOF-MS, matrix-assisted laser desorption/ionization time-of-flight mass spectrometry.

<sup>1</sup>Present address: Central Microscopy, Biology Center, University of Kiel, Ohlshausenstr. 40, D-24098 Kiel, Germany

differentiation, and neuronal growth (reviewed in Ichikawa and Hirabayashi, 1998); however, enzyme targets for GlcCer have not yet been identified. As with Cer, the subcellular distribution of endogenous GlcCer is not yet clear. A part of newly synthesized GlcCer is translocated from the cytosolic to the luminal site of the *cis*-Golgi for further glycosylation; however, a considerable portion of GlcCer is directly transported to the plasma membrane, where the main fraction (up to 45%) of cellular GlcCer is found (Klenk and Choppin, 1970; Jeckel *et al*, 1992; Warnock *et al*, 1993).

In the epidermis, Cer and GlcCer play a pivotal role in the maintenance of the epidermal permeability barrier. This barrier consists of a compact lipid matrix of Cer, free fatty acids and cholesterol embedded between the corneocytes in the stratum corneum (SC). GlcCer are the major precursors of epidermal Cer (Holleran *et al*, 1993). Both lipid families are transported to the SC by specialized secretory organelles, the lamellar bodies (LB). These are enriched in a polar lipid mixture of GlcCer, phospholipids, and sterols, and contain several acid hydrolases (Freinkel and Traczyk, 1985). At the transition of the stratum granulosum (SG) into the SC the LB fuse with the plasma membrane of the uppermost granular cell and extrude their contents into the intercellular space of the SC. Concomitantly, the polar lipids are enzymatically cleaved into the unpolar barrier lipids. The latter are arranged into multiple intercellular lipid lamellae, forming an efficient barrier against transcutaneous water loss (Elias and Menon, 1991; Forslind *et al*, 1997).

The epidermis is marked by a unique diversity of Cer and GlcCer species. To date, eight Cer and six GlcCer classes are known, the structures of which vary in the degree of hydroxylation of the sphingosine backbone and of the fatty acid (Fig 1). Among them there are two Cer and two GlcCer species that contain an  $\omega$ -hydroxy long chain fatty acid (C28–C34) (Wertz and Downing, 1983; Hamanaka *et al*, 1989; Robson *et al*, 1994; Stewart and Downing, 1999). The Cer with  $\omega$ -hydroxyacyl ( $\omega$ -OH-acyl) residues are known to be covalently bound to proteins of the cornified envelope of the corneocytes in the SC, thereby connecting the lipid matrix and the surrounding corneocytes (Marekov and Steinert, 1998). A corresponding covalently bound form of  $\omega$ -OH-acyl GlcCer has recently been identified in the epidermis of mice accumulating these lipids due to a defect in GlcCer catabolism (Doering *et al*, 1999a, b). As the amounts of the corresponding Cer were significantly reduced in these transgenic mice, it had been proposed that protein-bound GlcCer are at least in part direct precursors of the protein-bound Cer; however,

protein-bound GlcCer have not yet been identified in normal human epidermis.

Considering the multiple targets of Cer action and the essential role of GlcCer and Cer in epidermal homeostasis, it is of increasing interest to identify the subcellular localization of these lipids at the ultrastructural level. Recently, specific anti-sera against GlcCer and Cer have become commercially available. First applications of these sera in immunofluorescence staining of human epidermis have been reported (Brade *et al*, 2000; Vielhaber *et al*, 2001), but proof for the localization of Cer and GlcCer in epidermis by immunoelectron

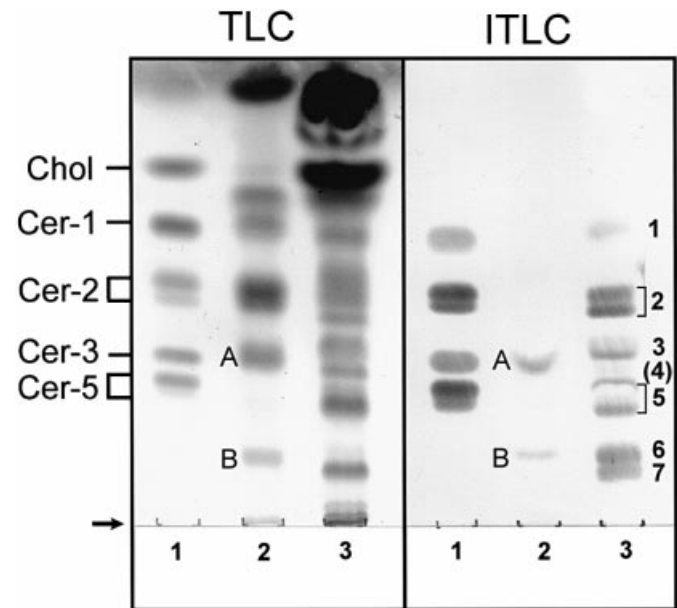
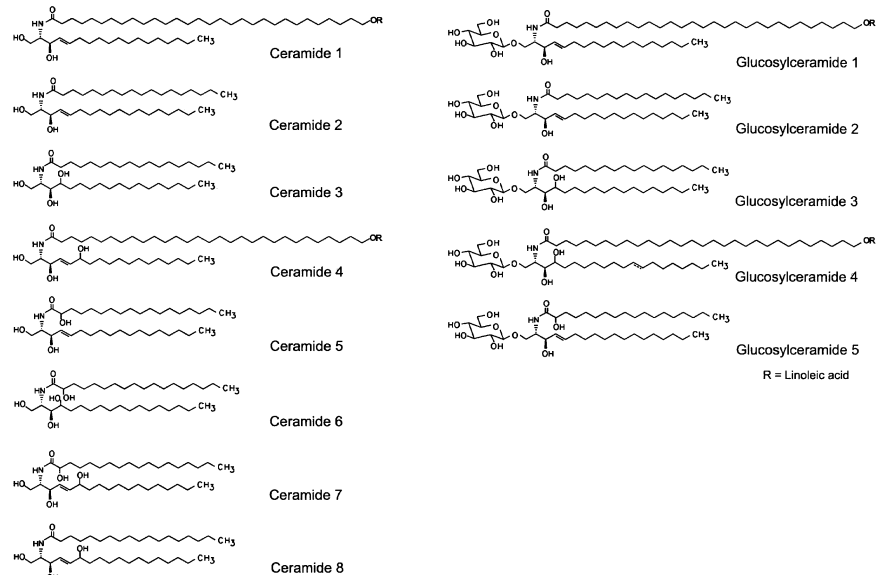


**Figure 2. Anti-Cer reacts with two covalently bound epidermal Cer in TLC immunostaining.** Aliquots of a standard lipid mixture (lane 1), lipids released by base hydrolysis from pre-extracted epidermis (lane 2) and an epidermal lipid extract (1.0 mg, lane 3) were separated by TLC and visualized with a spray reagent (TLC) or by immunostaining with mouse anti-Cer (ITLC), diluted 1 : 25. The standard lipid mixture was composed of cholesterol (Chol), Cer-1, Cer-2, Cer-3, and Cer-5 (8 nmol lipid each). (A) Cer A; (B) Cer B. The arrow indicates the origin.

**Figure 1. Structures of epidermal Cer and GlcCer.** According to Robson *et al* (1994) (Cer-1–Cer-7), Stewart and Downing, 1999) (Cer 8), Wertz and Downing (1983) (GlcCer-1–GlcCer-3, GlcCer-5), and Hamanaka *et al* (1989) (GlcCer-1, GlcCer-4). The position of the double bond in the sphingosine backbone of GlcCer-4 was not cleared up and is therefore indicated as a dashed line.



microscopy is still lacking. Here we show that the anti-sera react with both free and acylated  $\omega$ -OH-GlcCer and  $\omega$ -OH-Cer, respectively, and report on the ultrastructural localization of GlcCer and Cer in normal human epidermis.

## MATERIALS AND METHODS

**Anti-sera** The anti-GlcCer rabbit anti-serum and the IgM-enriched mouse anti-Cer anti-serum were a gift from GlycoTech Produktions- und Handelsgesellschaft mbH, Kuekels, Germany.

**Lipids** Cer-2 (ceramide type III) and Cer-5 (ceramide type IV), GlcCer-2, cholesterol, *N*-palmitoyl-D-sphingomyelin, phosphatidylethanolamine, and phosphatidylserine were purchased from Sigma (Taufkirchen, Germany). Cer-3 was obtained from Cosmoferm (Delft, the Netherlands). Cer-1 was chemically synthesized by R.R. Schmidt (University of Konstanz). Soybean GlcCer was isolated as described previously (Brade *et al.* 2000). In the same publication we had erroneously designated GlcCer-sb as GlcCer-3; however, MALDI-TOF mass spectrometric analysis (positive ion mode) of GlcCer-sb showed a major quasimolecular ion of  $m/z$  736.2  $[M + Na]^+$ , corresponding to a GlcCer containing a 2-hydroxypalmitic acid and a 4,8-sphingadienine backbone, which represents the main GlcCer species in soybean (Sullards *et al.* 2000). All substances were dissolved in chloroform/methanol (3:1, vol/vol).

**Isolation of covalently bound lipids** Epidermal lipid extracts from human breast skin were prepared as described by Doering *et al.* (1999a). For isolation of covalently bound Cer and GlcCer, the residual epidermal fragments were subjected to a further extraction, washed twice with 100% MeOH at room temperature and incubated in 95% MeOH for 1 h at 60°C. The pellet was repeatedly washed and incubated in warm MeOH until the supernatant was free of lipid [as judged from thin-layer chromatography (TLC) staining] before it was treated with 1 M KOH in 95% MeOH for 2 h at 40°C. Liberated lipids were recovered by two subsequent extractions of the supernatant.

**MALDI-TOF-MS** MALDI-TOF-MS of isolated soybean GlcCer (see *Lipids* section) and of covalently bound Cer and GlcCer was

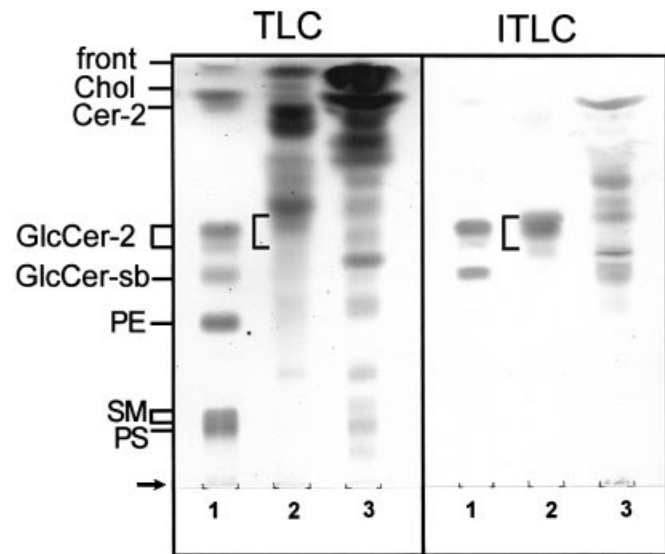


**Figure 3. Anti-GlcCer detects a covalently bound epidermal GlcCer species in TLC immunostaining.** Aliquots of a standard lipid mixture (lane 1), lipids released by base hydrolysis from pre-extracted epidermis (0.5 mg, lane 2) and an epidermal lipid extract (1.0 mg, lane 3) were separated by TLC and visualized with a spray reagent (TLC) or by immunostaining with rabbit anti-GlcCer (ITLC), diluted 1 : 1000. The standard lipid mixture was composed of cholesterol (Chol), Cer-2, GlcCer-2, GlcCer from soybean (GlcCer-sb), sphingomyelin (SM), phosphatidylethanolamine (PE), and phosphatidylserine (PS) (5 nmol lipid each). The bracket indicates the covalently bound GlcCer. In addition to the specific staining of GlcCer species, a cross-reaction with cholesterol occurred due to the high amounts of cholesterol present in the epidermal extract (lane 3). The arrow indicates the origin.

performed with a Bruker-Reflex III (Bruker-Franzen Analytik, Bremen, Germany) in linear and reflector TOF configuration at an acceleration voltage of 20 kV and delayed ion extraction. The compounds were

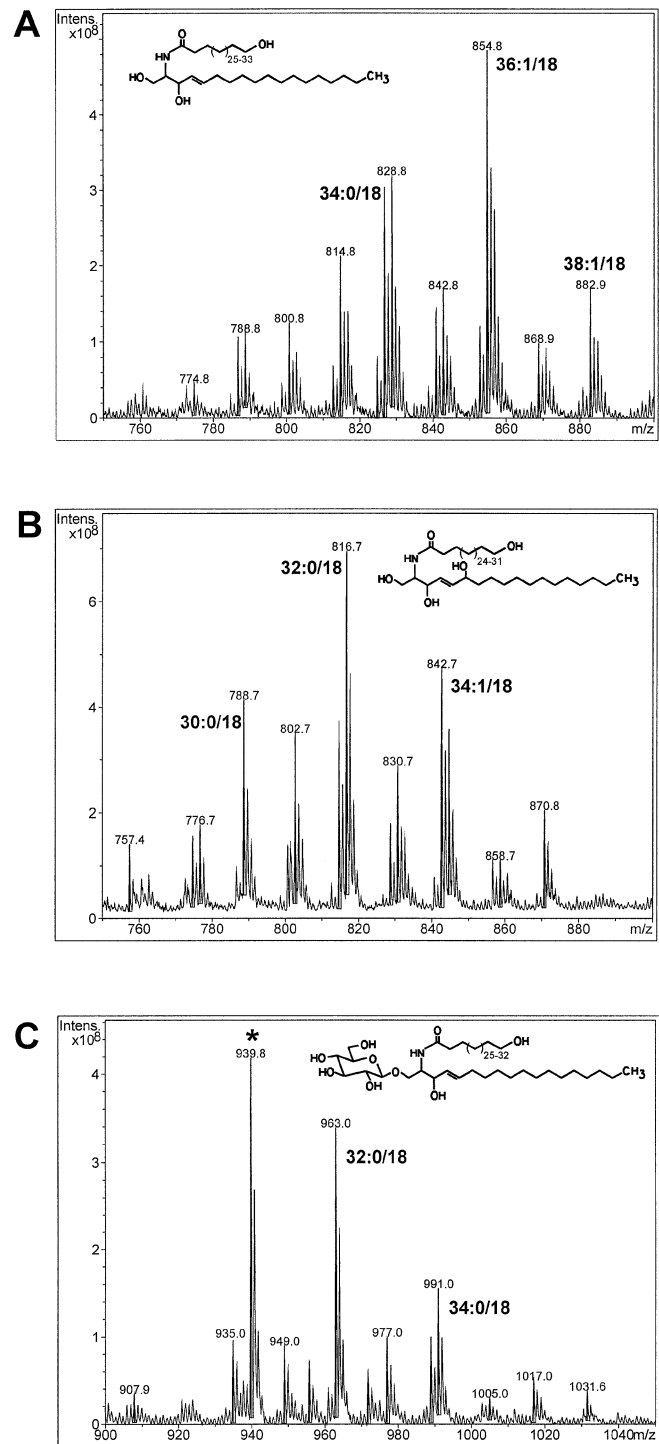
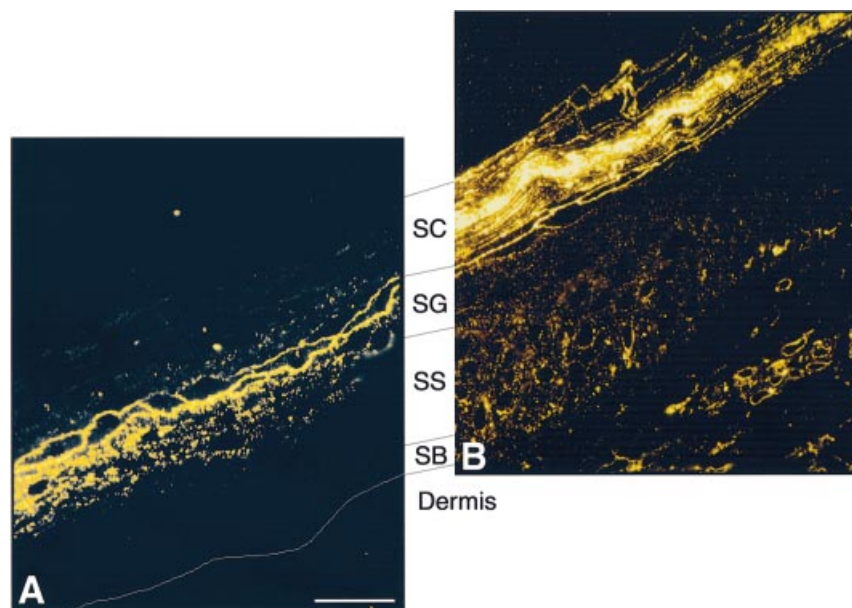


**Figure 4. MALDI-TOF-MS of covalently bound Cer and GlcCer.** Lipids were released from epidermis by alkaline hydrolysis, separated by TLC and subjected to TLC-immunostaining with anti-Cer (A,B) or anti-GlcCer (C). The immunoreactive bands were eluted from the silica gel of a nonstained TLC run in parallel. The indicated molecular masses represent positively charged sodium adducts of the respective molecules. The likely compositions of the predominant peaks are indicated with the carbon chain length of the fatty acid in the first position and that of the sphingosine base in the second position. The asterisk denotes an unidentified impurity from the silica gel.

**Figure 5. Localization of GlcCer and Cer in human epidermis by immunofluorescence microscopy.** Semithin sections of high-pressure frozen and freeze-substituted human skin, embedded in Lowicryl HM20, were stained with rabbit anti-GlcCer (A) and mouse anti-Cer (B) and Cy3-conjugated goat anti-rabbit IgG (A) or Cy3-conjugated goat anti-mouse IgM (B). The fine line in (A) indicates the epidermal-dermal junction. Scale bar: 20  $\mu$ m.



dissolved in  $\text{CHCl}_3/\text{CH}_3\text{OH}$  (50:50 vol/vol) at a concentration of 1  $\mu$ g per  $\mu$ l and vigorously vortexed. One microliter of the sample was then mixed with 1  $\mu$ l 0.5 M matrix solution of 2,5-dihydroxybenzoic acid (gentisic acid, DHB, Aldrich, Steinheim, Germany) in a 2:1 mixture of 0.1% trifluoroacetic acid/acetonitrile and aliquots of 0.5  $\mu$ l were deposited on a metallic sample holder and dried in a stream of air. The mass spectra shown are the average of at least 50 single analyses. Mass scale calibration was performed externally with similar compounds of known chemical structure.

**TLC and TLC immunostaining** Lipids were separated twice on silica gel 60 TLC plates with a solvent system of  $\text{CHCl}_3/\text{MeOH}/\text{CH}_3\text{COOH}$  (190:9:1 vol/vol/vol) and visualized by spraying with 10%  $\text{CuSO}_4$  and 8%  $\text{H}_3\text{PO}_4$  in water and heating at 180°C (Imokawa *et al.*, 1991). For separation of GlcCer, a third run in  $\text{CHCl}_3/\text{MeOH}/\text{NH}_4\text{OH}$  (65:35:5 vol/vol/vol) was performed. TLC immunostaining was performed as described previously (Brade *et al.*, 2000; Vielhaber *et al.*, 2001). Briefly, the plates were blocked with 0.1% nonfat dry milk/1% polyvinyl pyrrolidone in washing buffer (50 mM Tris/HCl, pH 7.4, 200 mM NaCl) and subsequently incubated overnight with rabbit-anti-GlcCer, diluted 1:1000 in blocking solution. After five washings bound antibody was detected by incubation with horseradish peroxidase-conjugated goat anti-rabbit IgG, diluted 1:1000 in blocking solution and following treatment with a mixture of 4-chloro-1-naphthol and hydrogen peroxide as the substrate. For immunostaining with anti-Cer the TLC plates were first incubated with 0.1% saponin in washing buffer, blocked with 5% nonfat dry milk in washing buffer and subsequently incubated with mouse serum against ceramide (1:25) in blocking solution. After five washings bound antibody was detected by incubation with horseradish peroxidase-conjugated goat anti-mouse IgM, diluted 1:1500 in blocking solution and developed as described for anti-GlcCer.

**Skin preparation for immunohistochemistry** Normal human skin biopsies obtained from human forearm were used in this study. Cryopreparation by high-pressure freezing and freeze substitution was carried out as described by Pfeiffer *et al.* (2000). Briefly, the skin specimens were placed in the cavity (100  $\mu$ m in depth) of a standard aluminum platelet filled with 1-hexadecene. The sandwich was inserted in the specimen holder and frozen in a high-pressure freezer (HPM 010 Bal-Tec, Balzers, FL; Müller and Moor, 1984). The subsequent freeze substitution (at -90°C for 30 h, -70°C for 8 h, -50°C for 8 h) was performed using acetone as substitution medium and uranyl acetate as fixing agent in a conventional freeze-substitution unit (FSU 010 Bal-Tec, Balzers, FL). Before cooling down to -90°C, the substitution medium was saturated with uranyl acetate at room temperature. The specimens were transferred directly to transfer vessels (Hohenberg *et al.*, 1994) and placed in 1.5 ml microfuge tubes (Eppendorf) filled with the substitution medium. After freeze substitution the skin specimens were infiltrated with methacrylate (HM20, Polysciences, Eppelheim, Germany) by the following protocol (at -50°C). Specimens were washed in pure

acetone for 30 min before infiltration with 30% (vol/vol) HM20/70% (vol/vol) acetone, and 70% HM20/30% acetone for 2 h, followed by three incubations for 2 h each in pure HM20. The ultraviolet polymerization was carried out at -50°C for 48 h followed by a postpolymerization at room temperature for at least 3 d.

**Immunohistochemistry** The following steps were performed at room temperature and all dilutions were prepared in washing buffer (phosphate-buffered saline/0.5% bovine serum albumin/0.2% fish gelatin).

For immunofluorescence, semithin sections (200 nm) were placed on glass coverslips, treated with normal goat serum (3% in phosphate-buffered saline) for 1 h, washed twice and incubated with anti-GlcCer-3 anti-serum (1:50) or with anti-Cer-anti-serum (1:2) for 1 h. Subsequently, the sections were washed four times and incubated with a Cy3-conjugated goat anti-rabbit IgG or goat anti-mouse IgM secondary antibody (Dianova, Hamburg, Germany) 1:800 for 1 h. The samples were washed six times, fixed on slides with MOWIOL and investigated with a Axioskop 35 fluorescence microscope (Zeiss, Jena, Germany). Image documentation was done with a Kodak Ektachrome 400 film.

Immunogold staining was performed on ultrathin sections (70 nm) as described for immunofluorescence except that the number of washing steps was doubled. For the double labeling experiments the primary and secondary antibodies were applied simultaneously. As secondary antibodies a goat anti-rabbit IgG (F(ab')<sub>2</sub> fragment) conjugated with 10 nm gold (anti-GlcCer) or a goat anti-mouse IgM ( $\mu$ -chain specific) conjugated with either 5 nm, 15 nm, or (in the double labeling experiments) 20 nm gold was used (each 1:50). Finally, the sections were poststained with uranyl acetate and investigated with a TEM912 $\Omega$  (LEO, Oberkochen, Germany). Digital image acquisition was performed with a CCD camera (ProScan, München, Germany). Image processing and statistical analysis were performed with the software AnalySIS 2.01 (Soft Imaging System, Münster, Germany).

## RESULTS

**Anti-Cer and anti-GlcCer react with very long chain  $\omega$ -OH epidermal Cer and GlcCer, respectively, in TLC immunostaining** In previous studies it had been demonstrated that the anti-sera against Cer and GlcCer used here for immunohistochemistry react with several epidermal Cer and GlcCer species, respectively, in TLC immunostaining (Brade *et al.*, 2000; Vielhaber *et al.*, 2001). Anti-Cer reacts strongly with Cer-2, Cer-5, and Cer-6, and to a lesser extent with Cer-1, Cer-3, and Cer-7 (Fig 2, lanes 1 and 3). A reaction with Cer-4 could not be detected, probably due to the low amounts of the lipid present in the epidermal extract. Anti-GlcCer reacts preferentially with GlcCer from soybean (GlcCer-sb), but also with human GlcCer-2 and some yet unidentified epidermal GlcCer species

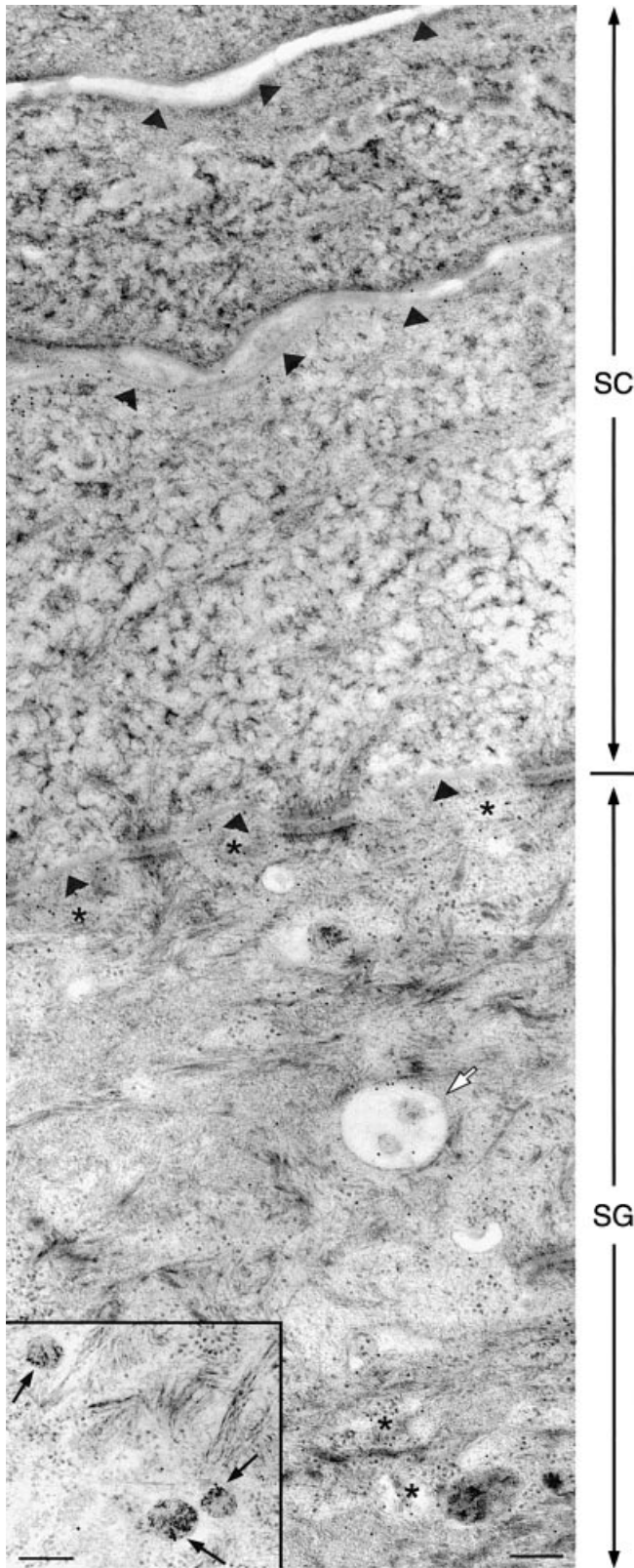


**Figure 6. GlcCer are localized at the cornified envelope of corneocytes in the lowermost SC layer.** Immunogold staining of GlcCer on ultrathin sections of cryoprocessed human skin, embedded in HM20. Overview of the SG and the lower SC. GlcCer were found in LB of the SS (*insert*) and of the SG (*asterisks*) as well as in TGN-like compartments (*white arrow*). Note the sharp decrease of labeling at the transition from the first to the second corneocyte layer. Scale bar: 250 nm.

(**Fig 3, lanes 1 and 3**); however, the reactivity with very long chain  $\omega$ -OH-Cer and  $\omega$ -OH-GlcCer that occur ester-linked to proteins of the cornified envelope had not so far been investigated. To ensure that the anti-sera are able to detect also these lipid species, the following TLC and ITLC experiments were done.

Human epidermis was subjected to exhaustive lipid extraction and subsequently treated with alkaline methanol to cleave off ester-linked lipids (Wertz *et al*, 1989). The liberated lipids were separated by TLC in parallel with a mixture of purified lipids and an untreated epidermal lipid extract and checked for lipid species reacting with anti-Cer (**Fig 2**) or anti-GlcCer (**Fig 3**). Anti-Cer reacted with two lipids of the fraction released by alkaline hydrolysis (**Fig 2, lane 2**), the molecular weight of which corresponded to the known protein-bound  $\omega$ -OH-Cer species, Cer A and Cer B, as determined by MALDI-TOF-MS (**Fig 4A, B**). In TLC immunostaining with anti-GlcCer one major and one minor band with  $R_f$  values similar to those of GlcCer-2 were stained in the extract of released covalently bound lipids (**Fig 3, lane 2**). The mass spectrometric analysis revealed that both bands represented a GlcCer with a ceramide portion corresponding to Cer A with fatty acid chain lengths from C30 up to C37 (**Fig 4C**); however, in accordance with Doering *et al* (1999a, b) we could not detect a GlcCer with a ceramide portion corresponding to Cer B.

Taken together, with the reaction of the two anti-sera with the majority of known epidermal Cer and GlcCer species, respectively, including very long chain  $\omega$ -OH-Cer and  $\omega$ -OH-GlcCer, the prerequisite for a representative immunohistochemical investigation on the ultrastructural distribution of Cer and GlcCer in epidermis was given.

#### **Anti-GlcCer staining concentrates in the SG, whereas anti-Cer preferentially stains the lower epidermis and the SC**

For all immunolight and immunoelectron microscopic experiments human epidermal samples were high-pressure frozen, freeze-substituted in acetone and embedded in Lowicryl HM20 (Pfeiffer *et al* 2000). This preparation method provides an excellent preservation of the ultrastructure and the proteinaceous antigenicity as well as an excellent lipid retention (Weibull *et al*, 1983; Humbel and Müller, 1984; Pfeiffer *et al*, 2000).

Immunofluorescence microscopy showed clearly that the two anti-sera did not cross-react with the respective heterologous antigen, as the anti-sera stained different epidermal sites (**Fig 5**). Anti-GlcCer stained exclusively the SG and upper SS, with an intracellular, vesicular pattern except in the uppermost SG where only the cell boundaries were stained (**Fig 5A**). No GlcCer were detected in the SC, in the lower epidermal layers or in the dermis. Interestingly, the immunofluorescence pattern of anti-GlcCer was nearly identical to that obtained by (O'Guin *et al*, 1989) with a monoclonal antibody directed against a protein associated with LB. In contrast, anti-Cer staining was concentrated at the cell membranes and/or the intercellular space in the SC and in the perinuclear region of the cells in the lower stratum spinosum (SS), the stratum basale (SB) and the dermis (**Fig 5B**). A faint staining was also observed at the cell periphery and/or the plasma membrane of the cells in the viable epidermis.

**GlcCer are localized in LB and at the membranes of trans-Golgi network (TGN)-like structures of the uppermost granular cells** In contrast to Cer, GlcCer were only detected in LB of the SG and the upper SS in immunoelectron microscopy (**Fig 6, asterisks**). In the uppermost layer of the SG, gold particles were observed within and at the membranes of closely arranged, large vesicles (**Fig 7**) that presumably represent TGN compartments. Those structures span a dense network throughout the cytoplasm of the uppermost SG cells (Elias *et al*, 1998).

The GlcCer staining was most intense at the transition of the SG to the SC. Upon fusion of the LB with the plasma membrane of the uppermost granular cells, GlcCer were found at the cornified envelope (**Fig 7, arrowheads**) of the cells in the first SC layer, which appeared as a homogeneous, electron dense layer on the surface of the corneocytes. In the second SC layer, the staining sharply

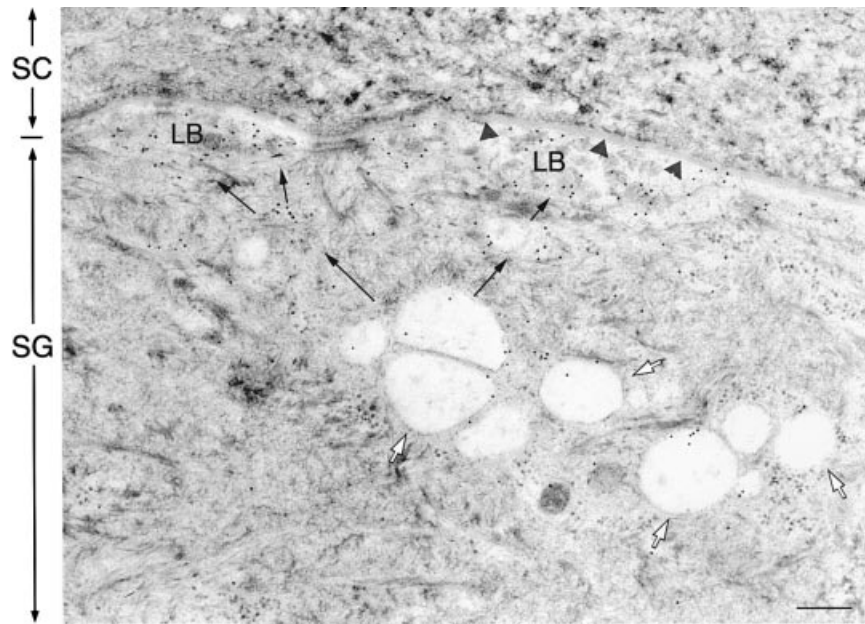


**Figure 7. GlcCer is secreted to the SG/SC interface via LB that derive from TGN-like compartments.** Immunogold staining of GlcCer on ultrathin sections of cryoprocessed human skin, embedded in HM20. Cell at the SG/SC transition. GlcCer is transported from TGN-like compartments (white arrows) via LB to the plasma membrane of the uppermost granular cells. Note the staining of the cornified envelope (arrowheads). Scale bar: 250 nm.

decreased (Fig 6). No labeling was observed in the higher SC layers.

**In the lower epidermis, Cer is located at membranes of the ER, the Golgi, the nucleus, mitochondria, and at the plasma membrane** Immunoelectron microscopy with anti-Cer revealed two separate pools of Cer. One of which was located in the SB and lower SS where four preferred localizations could be distinguished: (i) the ER and the Golgi apparatus; (ii) the nuclear envelope; (iii) the inner and outer mitochondrial membranes; and (iv) the plasma membrane (Fig 8). In addition, multivesicular bodies occasionally showed gold particles (data not shown). This staining pattern disappeared in the more differentiated cells. In the SG, a staining of the mentioned organelles was found only very rarely. Quantitation of the number of gold particles per membrane length of the different organelles in the cells of the SB revealed that the labeling was most dense on mitochondrial membranes compared with the nuclear membrane, the ER, the Golgi, and the plasma membrane with respective ratios of 11.9:4.6:3.6:3.7:1 (Table I). Interestingly, Cer labeling on the nuclear envelope was preferentially localized to the inner nuclear membrane with a ratio of 3.0 ( $n = 35$ ) relative to the outer nuclear membrane.

For estimation of the inner mitochondrial membrane length we referred to the work of Schwerzmann *et al* (1986) who found that in rat liver mitochondria the areas of the inner mitochondrial membrane was threefold larger than that of the outer membrane.

The area ratio of the mitochondrial membranes might differ in epidermal cells; however, even if the ratio of the outer to the inner membrane area was supposed to be 1:1 (corresponding to a total mitochondrial membrane labeling density of  $11.1 \pm 0.56$  gold particles per  $\mu\text{m}$ ) or 1:4 (corresponding to  $16.64 \pm 0.84$  gold particles per  $\mu\text{m}$ )—in every case the mitochondria remained the most densely labeled organelles.

**In the upper epidermis, Cer are localized in LB, in the intercellular space and at the cornified envelope** The second pool of Cer was localized in the uppermost layer of the epidermis, showing gold particles arrayed like a string of pearls along the cornified envelope (Fig 9A) and in the intercellular space of the SC (Fig 9B, C). As expected, Cer labeling was also localized in the LB

at the interface of the SC and the SG (Fig 9D). Finally, a prominent labeling was found in all LB upon their nascence in the SS up to the uppermost SG (Fig 10). In addition, Cer staining in the SS was found in vesicular organelles and at the plasma membrane. In the SS and predominantly in the SG Cer was localized in larger, vesicular structures, which probably represent TGN compartments (white arrows in Fig 10). LB were often found in close proximity to TGN-like structures, many of which were present especially in the uppermost SG layer (Fig 7).

In control experiments without the primary antibodies only occasionally gold particles were observed that were randomly distributed over the whole section (data not shown).

## DISCUSSION

Cer and GlcCer are important biologic effector molecules. In the epidermis, they fulfill an essential role as structural components of the epidermal permeability barrier. There is a range of data from biochemical analyses on the distribution of both sphingolipids in the different epidermal layers, whereas the subcellular compartmentalization of Cer and GlcCer has not yet been elucidated in detail. With the aid of two new anti-sera against Cer and GlcCer, respectively, and an optimized cryopreparation method for transmission electron microscopy of human epidermis, it became possible to investigate the subcellular distribution of GlcCer and Cer in cryoprocessed human epidermis by immunoelectron microscopy.

In this study we first assured by TLC immunostaining that both antibodies do not only react with free epidermal Cer and GlcCer, but also with very long chain  $\omega$ -OH-Cer and  $\omega$ -OH-GlcCer liberated from the epidermis by alkaline hydrolysis. Thus, the prerequisite for a representative immunohistochemical study on the subcellular distribution of Cer and GlcCer was given. Using immunofluorescence and immunoelectron microscopy we showed that Cer are localized in dermal and basal epidermal cells in mitochondria, at the nuclear envelope, at the plasma membrane, at the ER, and at the Golgi complex. In the upper epidermis, Cer were found in LB, in the intercellular space of the SC, and at the cornified envelope of the corneocytes. GlcCer were exclusively

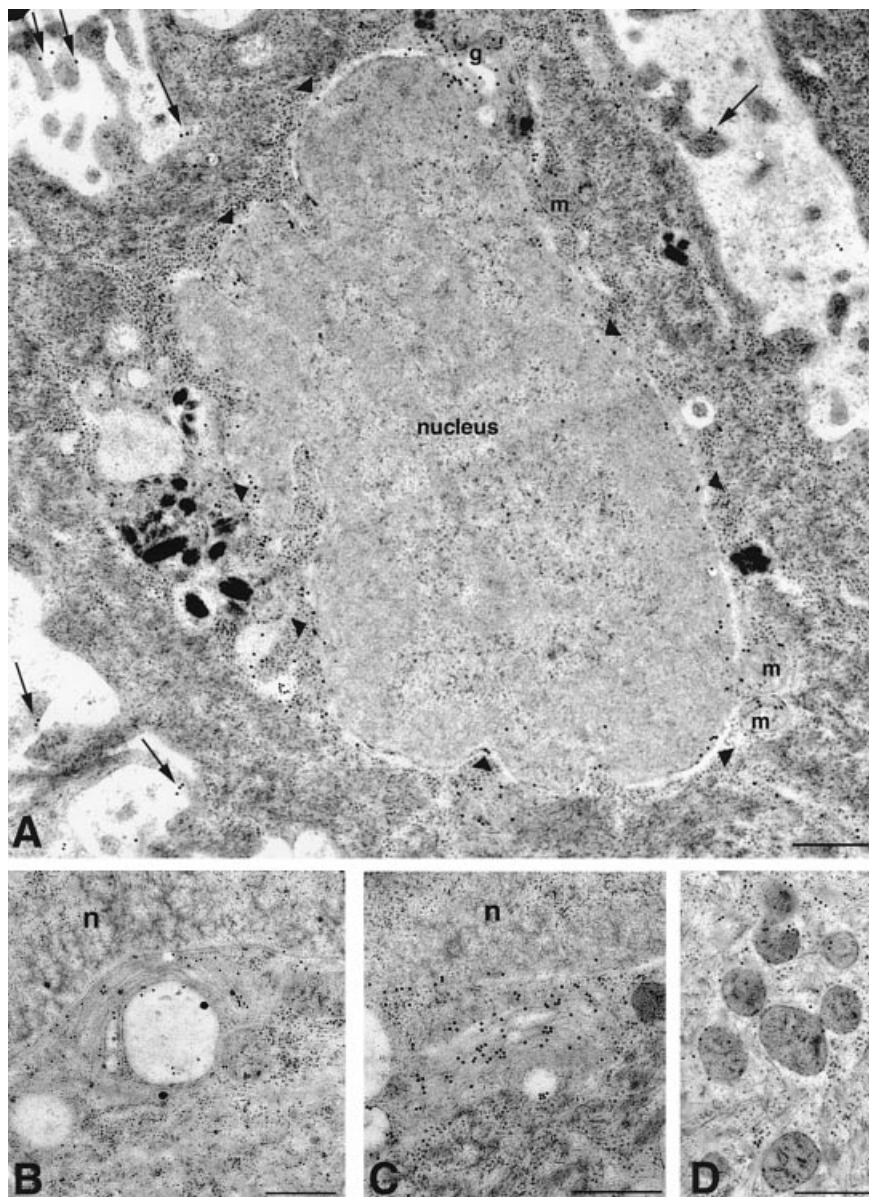


**Figure 8. Ultrastructural localization of Cer in basal human epidermal cells.** Immunogold staining of Cer on ultrathin sections of cryoprocessed human skin, embedded in HM20. Cer staining (15 nm gold) was found preferentially (A) at the nuclear membrane (B) on the ER and (C) Golgi membranes, and (D) in mitochondria. g, Golgi apparatus; m, mitochondrion; n, nucleus; arrowheads, nuclear membrane; arrows, plasma membrane. Scale bar: 500 nm.

detected in LB and at the cornified envelope of the lowermost corneocytes.

The immunofluorescence staining patterns obtained with anti-Cer and anti-GlcCer generally showed a good correlation with the known lipid analytical data; however, there was a lack of GlcCer staining in the lower epidermis. The Cer and GlcCer content of human epidermis changes from 4% (Cer)/3.5% (GlcCer) of the total lipid weight in the basal and spinous layers and 9%/6% in the granular layer to 25%/traces in the SC (Lampe *et al*, 1983). On a molar weight basis, the Cer content exceeds that of GlcCer 2-fold in the SB/SS, 2.5-fold in the SG, and 31-fold in the SC. Thus, the cellular amounts of the named sphingolipids in the lower epidermis might be sufficient for the detection of Cer, but not for that of GlcCer. A high local concentration of such a small antigen is a prerequisite for its detection in immunohistochemistry, and in the case of GlcCer, this is presumably only given in the LB.

The immunoelectron microscopic investigation revealed a concentration of Cer in the mitochondria of basal epidermal and dermal cells, suggesting an important role for Cer in these organelles. This hypothesis is supported by the growing evidence for a participation of ceramide in the regulation of mitochondrial

function (Ghafourifar *et al*, 1999; Di Paola *et al*, 2000) and the recent identification of a mitochondrial ceramidase (El Bawab *et al*, 2000). Moreover, the presence of Cer in mitochondria correlates with previous observations made by Lipsky and Pagano (1983), who incubated Chinese hamster fibroblasts with liposomes containing the fluorescent Cer-analog C6-NBD-Cer at 2°C. They detected 90% of the fluorescent lipid within mitochondria, whereas the residual 10% were found at the nuclear envelope and the ER. Upon warming up the cells to 37°C, the fluorescence rapidly associated with the Golgi complex, where C6-NBD-Cer was further metabolized to glycosphingolipid analogs.

In addition, a significant portion of cellular ceramide was found at the nuclear envelope, obviously reflecting the biosynthetic site of Cer at the ER; however, statistical analysis revealed that Cer were preferentially localized at the inner nuclear membrane. The presence of a nuclear pool of Cer provides support for previous assumptions of an involvement of Cer in apoptotic events occurring at or in the nucleus. Recently, increased neutral sphingomyelinase and ceramidase activities have been measured in purified nuclei from rat hepatocytes after induction of apoptosis by portal vein branch

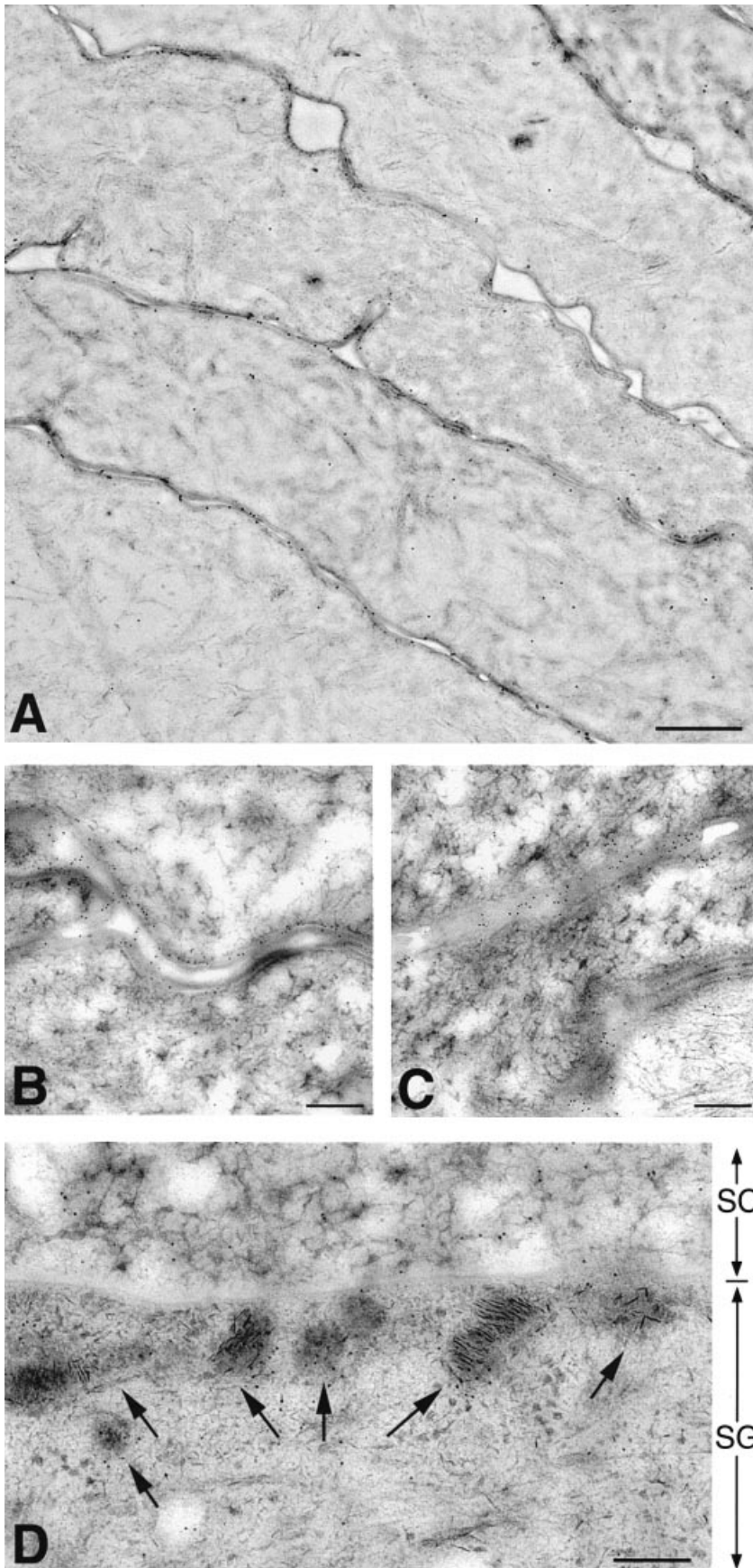


**Figure 9. Ultrastructural localization of Cer in the upper epidermis.** Immunogold staining of Cer on ultrathin sections of cryoprocessed human skin, embedded in HM20. (A) Corneocytes were stained along the cornified envelope (15 nm gold). (B) If the intercellular space of the SC was free of biological material, Cer (5 nm gold) were concentrated on the corneocytes surface. (C) Cer staining (5 nm gold) was found mainly intercellularly, if the intercellular space was filled with biological material. (D) LB (arrows) at the SG/SC transition zone were labeled with anti-Cer (5 nm gold). Scale bar: (A) 1 μm; (B–D) 200 nm.

ligation in the liver (Tsugane *et al*, 1999). It had been suggested that Cer are generated at the inner leaflet of the nuclear envelope (Hoekstra, 1999). In this context, it is interesting to

note that the proteinaceous apoptotic inhibitor bcl-2 is localized in the same compartments as Cer with the exception of the Golgi apparatus and the plasma membrane (Akao *et al*, 1994).

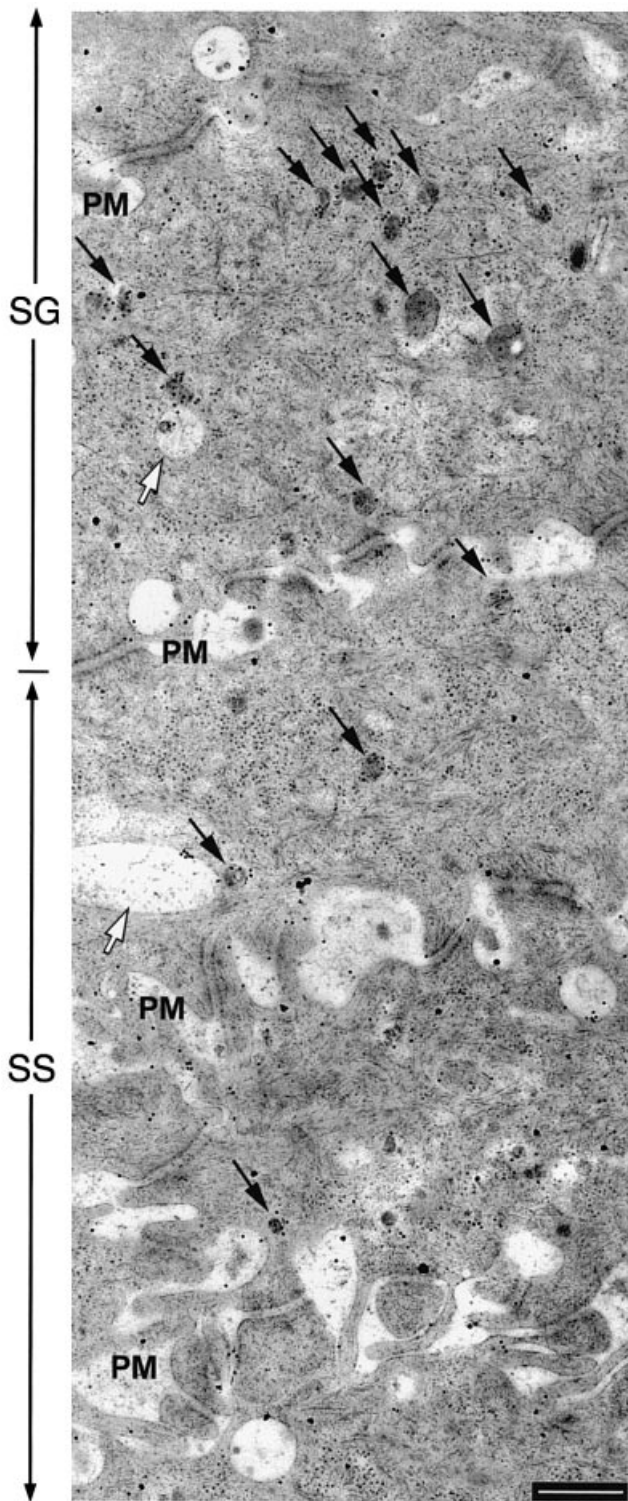


**Figure 10. Cer are transported to the SC via LB.** Immunogold staining of Cer (15 nm gold) on ultrathin sections of cryoprocessed human skin, embedded in HM20. Cer were predominantly localized in LB (arrows) in the SS and the SG, but also at the plasma membrane and in vesicular organelles (white arrows). In their close proximity LB were often observed. Note that the number of LB continuously increases with ongoing epidermal differentiation. Scale bar: 500 nm.

The second main Cer fraction was located in the upper epidermis, where Cer were found in all LB from their nascence in the mid to upper SS up to the uppermost SG and at the cornified

**Table I. Labeling densities of ceramide in organelles of basal epidermal cells<sup>a</sup>**

Compartment	Labeling density (gold particles/membrane length)
Nuclear envelope	5.66 ± 0.32/μm (n = 39)
Plasma membrane	1.24 ± 0.18/μm (n = 20)
ER	4.44 ± 0.49/μm (n = 16)
Golgi	4.57 ± 0.45/μm (n = 10)
Mitochondria <sup>b</sup> (outer + inner membrane)	14.71 ± 0.77/μm (n = 89)
Nucleoplasm (background)	0.46 ± 0.13/μm (n = 16)

<sup>a</sup>The membrane length was determined with the aid of the analySIS software at a magnification of ×28,000. The values of labeling density are expressed as the mean value ± SEM. The number of compartments counted is given in brackets. The number of gold particles (15 nm) counted was 1743.

<sup>b</sup>The length of the inner mitochondrial membrane ( $m_i$ ) was calculated on the basis of the assumption that the area of  $m_i$  is about 3-fold larger than the area of  $m_o$  (Schwerzmann *et al*, 1986). Thus, the length of  $m_i$  corresponds to  $\sqrt{3} * m_o$ .

envelope, indicating that Cer are incorporated into LB upon their biogenesis. Interestingly, in contrast to the prominent labeling of the TGN-like compartments, neither Cer nor GlcCer labeling was found in the Golgi apparatus of the upper SS and the SG, underlining the functional distinctness of the Golgi and the TGN in the upper epidermis (Man *et al*, 1995; Elias *et al*, 1998). Together with the accumulation of NBD-Cer in the TGN of the outermost SG cell layer in three-dimensional organotypic cultures (Elias *et al*, 1998) and the lack of Cer labeling at the nuclear membrane and in mitochondria in the upper epidermal cell layers, these data suggest that the activity of Cer metabolism in the differentiated epidermis is concentrated to the TGN and LB.

In the SC, Cer labeling was concentrated at the cornified envelope, whereas labeling of the intercellular space was only rarely detected; however, mechanical stress during removal of the punch itself and of the skin biopsy from the punch often causes widening of the intercellular space in the SC, leading to large intercellular areas of up to 1 μm in the mid and upper SC (Fig 9A). These areas were free of biological material, and the lipids were concentrated near the corneocyte surface. In regions where the intercellular space is filled with biologic material, especially in the lower SC, we detected Cer mainly intercellularly (Fig 9C).

Intercellular membranes in the SC, however, were not detectable in the labeled sections. From our experience, the multiple incubation steps during immunolabeling resulted in a blurring of the lipid lamellae structure. This is caused by a loss of the contrasting agent uranyl acetate during exposure of the section surface to the aqueous solutions as uranyl acetate does not covalently bind but only associates to the skin lipids. Therefore, we shortened the immunolabeling protocol to a minimum (about 4 h in total still gave a good signal-to-background ratio). Nevertheless, whereas uranyl acetate is extracted, the lipids are retained in the section and can be visualized by immunolabeling.

Finally, it is important to note that precise Cer and GlcCer immunohistochemical localization can only be performed with specimens dehydrated at temperatures below -50°C and embedded into Lowicryl resins with subsequent ultraviolet light polymerization at -50°C to minimize the loss of lipids (Weibull *et al*, 1983), as already stated in preceding publications (Brade *et al*, 2000; Vielhaber *et al* in press). With the use of uranyl acetate as the sole fixative during freeze substitution the extraction of lipids is further reduced (Humbel and Müller, 1984; Pfeiffer *et al*, 2000).

Our finding of a GlcCer labeling in closely arranged, large vesicles that probably represent TGN compartments correlates well with previous investigations: Elias *et al* (1998) demonstrated

that the uppermost granular cells are filled up with TGN membranes, appearing as a tubuloreticular structure. The latter could be labeled with the Golgi-specific fluorescent Cer analog NBD-Cer. In addition, Madison and Howard, 1996) showed by NBD-Cer labeling that in differentiated keratinocyte cultures Cer are transported through the Golgi apparatus, where they are further metabolized into GlcCer and transported to the plasma membrane by a vesicular mechanism. Later, the same group provided additional evidence for a Golgi origin of LB via the correlation of increasing ceramide glucosyltransferase activity with differentiation, GlcCer amount, and LB formation (Madison *et al*, 1998).

The immunoelectron microscopical investigations with anti-GlcCer demonstrated that GlcCer are secreted via LB into the intercellular space of the SC and then associate with the cornified envelope of the cells in the first corneocyte layer. Together with the detection of a covalently bound GlcCer species by TLC immunostaining and in agreement with studies in transgenic mice (Doering *et al*, 1999a, >b), our data support the significance of these unique glycoconjugates as precursors for protein-bound Cer.

The concentration of endogenous Cer in mitochondria and at the nuclear envelope demands further investigations into the role of endogenous Cer at these sites. The combination of biochemical analyses and Cer immunoelectron microscopy will provide a powerful tool to elucidate further the relationship of Cer with the various signal transduction pathways. Finally, it will be of special interest for dermatologists to analyze the ultrastructural distribution of GlcCer and, in particular, Cer in pathologic epidermis with a disturbed barrier function as, for example, in atopic dry skin or ichthyotic skin.

We thank N. Hamel for excellent technical assistance, O. Brandt for providing samples of human skin, and H. Brade, G. Griffiths, and T. Doering for critically reading the manuscript.

## REFERENCES

- Akao Y, Otsuki Y, Kataoka S, Ito Y, Tsujimoto Y: Multiple subcellular localization of bcl-2: detection in nuclear outer membrane, endoplasmic reticulum membrane, and mitochondrial membranes. *Cancer Res* 54:2468-2471, 1994
- Brade L, Vielhaber G, Heinz E, Brade H: In vitro characterization of anti-glucosylceramide rabbit antisera. *Glycobiology* 10:629-636, 2000
- Chalfant CE, Kishikawa K, Mumby MC, Kamibayashi C, Bielawska A, Hannun YA: Long chain ceramides activate protein phosphatase-1 and protein phosphatase-2A. Activation is stereospecific and regulated by phosphatidic acid. *J Biol Chem* 274:20313-20317, 1999
- Di Paola M, Cocco T, Lorusso M: Ceramide interaction with the respiratory chain of heart mitochondria. *Biochemistry* 39:6660-6668, 2000
- Doering T, Proia RL, Sandhoff K: Accumulation of protein-bound epidermal glucosylceramides in  $\beta$ -glucocerebrosidase deficient type 2 Gaucher mice. *FEBS Lett* 447:167-170, 1999a
- Doering T, Holleran WM, Potratz A, Vielhaber G, Suzuki K, Elias PM, Sandhoff K: Sphingolipid activator proteins (SAPs) are required for epidermal permeability barrier formation. *J Biol Chem* 274:11038-11045, 1999b
- El Bawab S, Roddy P, Qian T, Bielawska A, Lemasters JJ, Hannun YA: Molecular cloning and characterization of a human mitochondrial ceramidase. *J Biol Chem* 275:21508-21513, 2000
- Elias PM, Menon GK: Structural and lipid biochemical correlates of the epidermal permeability barrier. *Adv Lipid Res* 33:301-313, 1991
- Elias PM, Cullander C, Mauro T, Rassner U, Kömüves L, Brown BE, Menon GK: The specialized granular cell: the outermost granular cell as a specialized secretory cell. *J Invest Dermatol Symp Proc* 3:87-100, 1998
- Forslind B, Engström S, Engblom J, Norlén L: A novel approach to the understanding of human skin barrier function. *J Dermatol Sci* 14:115-125, 1997
- Freinkel RK, Traczyk TN: Lipid composition and acid hydrolase content of lamellar granules of fetal rat epidermis. *J Invest Dermatol* 85:295-298, 1985
- Geilen C, Wieder T, Orfanos CE: Ceramide signalling, regulatory role in cell proliferation, differentiation and apoptosis in human epidermis. *Arch Dermatol Res* 289:559-566, 1997
- Ghafourifar P, Klein SD, Schucht O, Schenk U, Pruschy M, Rocha S, Richter C: Ceramide induces cytochrome C release from isolated mitochondria. *J Biol Chem* 274:6080-6084, 1999
- Hamanaka S, Asagami C, Suzuki M, Inagaki F, Suzuki A: Structure determination of Glc $\beta$ -1-N-( $\omega$ -O-linoleoyl)-acylsphingosines of human epidermis. *J Biochem* 105:684-690, 1989
- Heinrich M, Wickel M, Schneider-Brachert W, *et al*: Cathepsin D targeted by acid sphingomyelinase. *EMBO J* 18:5252-5263, 1999
- Hoekstra D: Ceramide-mediated apoptosis of hepatocytes in vivo: a matter of the nucleus? *J Hepatol* 31:161-164, 1999
- Hohenberg H, Mannweiler K, Müller M: High-pressure freezing of cell suspensions in cellulose capillary tubes. *J Microscopy* 175:34-43, 1994
- Holleran WM, Takagi Y, Menon GK, Legler G, Feingold KR, Elias PM: Processing of epidermal glucosylceramide is required for optimal mammalian cutaneous permeability function. *J Clin Invest* 91:1656-1664, 1993
- Humbel BM, Müller M: Freeze substitution and low temperature embedding. In: Müller M, Becker PR, Boyde A, Wolosewick, JJ (eds). *The Science of Biological Specimen Preparation*. Scanning Electron Microscopy Inc., AFM O'Hara, Dr Om Jahari, Chicago, IL, 1985, pp 175-183
- Huwiler A, Brunner J, Hummel R, Vervoordeldonk M, Stabel S, van den Bosch H, Pfeilschifter J: Ceramide-binding and activation defines protein kinase c-Raf as a ceramide-activated protein kinase. *Proc Natl Acad Sci USA* 93:6959-6963, 1996
- Ichikawa S, Hirabayashi Y: Glucosylceramide synthase and glycosphingolipid synthesis. *Trends Cell Biol* 8:198-202, 1998
- Imokawa G, Abe A, Kumi J, Higaki Y, Kawashima M, Hidano A: Decreased level of ceramides in stratum corneum of atopic dermatitis: an etiologic factor in atopic dry skin? *J Invest Dermatol* 96:523-526, 1991
- Jeckel D, Karrenbauer A, Burger KN, van Meer G, Wieland F: Glucosylceramide is synthesized at the cytosolic surface of various Golgi subfractions. *J Cell Biol* 117:259-267, 1992
- Klenk H-D, Chopin PW: Glycosphingolipids of plasma membranes of cultured cells and an enveloped virus (SV5) grown in these cells. *Proc Natl Acad Sci USA* 66:57-64, 1970
- Lampe MA, Williams ML, Elias PM: Human epidermal lipids, characterization and modulations during differentiation. *J Lipid Res* 24:131-140, 1983
- Lavie Y, Cao H, Bursten SL, Giuliano AE, Cabot MC: Accumulation of glucosylceramides in multidrug-resistant cancer cells. *J Biol Chem* 271:19530-19536, 1996
- Levade T, Jaffrézou J-P: Signalling sphingomyelinases. which, where, how and why? *Biochim Biophys Acta* 1438:1-17, 1999
- Lipsky NG, Pagano RE: Sphingolipid metabolism in cultured fibroblasts. microscopic and biochemical studies employing a fluorescent ceramide analogue. *Proc Natl Acad Sci USA* 80:2608-2612, 1983
- Lipsky NG, Pagano RE: A vital stain for the Golgi apparatus. *Science* 228:745-747, 1985
- Lucci A, Cho WI, Han TY, Giuliano AE, Morton DL, Cabot MC: Glucosylceramide: a marker for multiple-drug resistant cancers. *Anticancer Res* 18:475-480, 1998
- Madison KC, Howard EJ: Ceramides are transported through the Golgi apparatus in human keratinocytes *in vitro*. *J Invest Dermatol* 106:1030-1035, 1996
- Madison KC, Sando GN, Howard EJ, True CA, Gilbert D, Swartzendruber DC, Wertz PW: Lamellar granule biogenesis. a role for ceramide glucosyltransferase, lysosomal enzyme transport, and the Golgi. *J Invest Dermatol Symp Proc* 3:80-86, 1998
- Man MQ, Brown BE, Wu-Pong S, Feingold R, Elias PM: Exogenous nonphysiologic vs. physiologic lipids. Divergent mechanisms for correction of permeability barrier dysfunction. *Arch Dermatol* 131:809-816, 1995
- Marekov LN, Steinert PM: Ceramides are bound to structural proteins of the human foreskin epidermal cornified envelope. *J Biol Chem* 273:17763-17770, 1998
- Müller M, Moor H: Cryofixation of thick specimens by high-pressure freezing. In: Revel JP, Barnad T, Haggis GH (eds). *The Science of Biological Specimen Preparation for Microscopy and Microanalysis*. Scanning Electron Microscopy Inc., AFM O'Hara, Dr Om Jahari, Chicago, IL, 1983, pp 131-138
- Müller G, Ayoub M, Storz P, Rennecke J, Fabbro D, Pfizenmaier K: PKC zeta is a molecular switch in signal transduction of TNF- $\alpha$ , bifunctionally regulated by ceramide and arachidonic acid. *EMBO J* 14:1961-1969, 1995
- O'Guin WM, Manabe M, Sun T-T: Association of a basic 25K protein with membrane coating granules of human epidermis. *J Cell Biol* 109:2313-2321, 1989
- Perry DK, Hannun YA: The role of ceramide in cell signalling. *Biochim Biophys Acta* 1436:233-243, 1998
- Pfeiffer S, Vielhaber G, Vietzke J-P, Witterm K-P, Hintze U, Wepf R: High-pressure freezing provides new information on human epidermis: simultaneous protein antigen and lamellar lipid structure preservation. Study of human epidermis by cryoimmunoblotting. *J Invest Dermatol* 114:1030-1038, 2000
- Robson KJ, Stewart ME, Michelsen S, Lazo ND, Downing DT: 6-Hydroxy-4-sphingene in human epidermal ceramides. *J Lipid Res* 35:2060-2068, 1994
- Rosenwald AG, Pagano RE: Intracellular transport of ceramide and its metabolites at the Golgi complex: Insights from short-chain analogs. *Adv Lipid Res* 26:101-118, 1993
- Schwerzmann K, Cruz-Orive LM, Eggman R, Sängner A, Weibel ER: Molecular architecture of the inner membrane of mitochondria from rat liver: a combined biochemical and stereological study. *J Cell Biol* 102:97-103, 1986
- Stewart ME, Downing DT: A new 6-hydroxy-4-sphingene-containing ceramide in human skin. *J Lipid Res* 40:1434-1439, 1999
- Sullards MC, Lynch DV, Merrill AH, Adams J: Structure determination of soybean and wheat glucosylceramides by tandem mass spectrometry. *J Mass Spectrom* 35:347-353, 2000
- Tsugane T, Tamiya-Koizumi K, Nagino M, Nimura Y, Yoshida S: A possible role of nuclear ceramide and sphingosine in hepatocyte apoptosis in rat liver. *J Hepatol* 31:8-17, 1999
- Van Echten-Deckert G, Klein A, Linke T, Heinemann T, Weisgerber J, Sandhoff K:

- Turnover of endogenous ceramide in cultured normal and Farber fibroblasts. *J Lipid Res* 38:2569-2579, 1997
- Vielhaber G, Brade L, Lindner B, et al: Mouse anti-ceramide antiserum. A specific tool for the detection of endogenous ceramide. *Glycobiology* 11:451-457, 2001
- Warnock DE, Roberts C, Lutz MS, Blackburn WA, Young WW, Baenziger JU: Determination of plasma membrane lipid mass and composition in cultured Chinese hamster ovary cells using high gradients magnetic affinity chromatography. *J Biol Chem* 268:10145-10153, 1993
- Weibull CA, Christiansson A, Carlemalm E: Extraction of membrane lipids during fixation, dehydration and embedding of *Acholeplasma laidlawi* cells for electron microscopy. *J Microscopy* 129:201-207, 1983
- Wertz PW, Downing DT: Glucosylceramides of pig epidermis: structure determination. *J Lipid Res* 24:1135-1139, 1983
- Wertz PW, Madison KC, Downing DT: Covalently bound lipids of human stratum corneum. *J Invest Dermatol* 92:109-111, 1989
- Zhang Y, Yao B, Delikat S, et al: Kinase suppressor of Ras is ceramide-activated protein kinase. *Cell* 89:63-72, 1997